DOI:
10.1021/acsnano.9b04898

Document Version
Other version

- Supporting Information -

Neutron Activated ^{153}Sm Sealed in Carbon Nanocapsules for *In Vivo* Imaging and Tumor Radiotherapy

Julie T.-W. Wang[a], Rebecca Klippstein[a], Markus Martincic[b], Elzbieta Pach[c], Robert Feldman[d], Martin Šefl[e,f], Yves Michel[d], Daniel Asker[a], Jane K. Sosabowski[g], Martin Kalbac[h], Tatiana Da Ros[i], Cécilia Ménard-Moyon[j], Alberto Bianco[j], Ioanna Kyriakou[e], Dimitris Emfietzoglou[e], Jean-Claude Saccavini[d], Belén Ballesteros[c,], Khuloud T. Al-Jamal[a,]* and Gerard Tobias[b,]**

[a]Institute of Pharmaceutical Science, King's College London, London SE1 9NH, UK

[b]Institut de Ciència de Materials de Barcelona (ICMAB-CSIC), Campus UAB, 08193 Bellaterra, Barcelona, Spain

[c]Catalan Institute of Nanoscience and Nanotechnology (ICN2), CSIC and the Barcelona Institute of Science and Technology, Campus UAB, 08193 Bellaterra, Barcelona, Spain

[d]Cis Bio International Ion Beam Applications SA, Gif sur Yvette 91192, France

[e]Medical Physics Laboratory, University of Ioannina Medical School, Ioannina GR-45110, Greece

[f]Faculty of Nuclear Sciences and Physical Engineering, Czech Technical University in Prague, Prague 11519, Czech Republic

[g]Centre for Molecular Oncology, Barts Cancer Institute, Queen Mary University of London, London EC1M 6BQ, UK

[h]J. Heyrovsky Institute of the Physical Chemistry, Dolejskova 3, 182 23 Prague 8, Czech Republic

[i]INSTM Unit of Trieste, Department of Chemical and Pharmaceutical Sciences, University of Trieste, Via L. Giorgieri 1, 34127 Trieste, Italy

[j]University of Strasbourg, CNRS, Immunology, Immunopathology and Therapeutic Chemistry, UPR 3572, 67000 Strasbourg, France.

*Corresponding authors E-mail: gerard.tobias@icmab.es, khuloud.al-jamal@kcl.ac.uk, belen.ballesteros@icn2.cat.

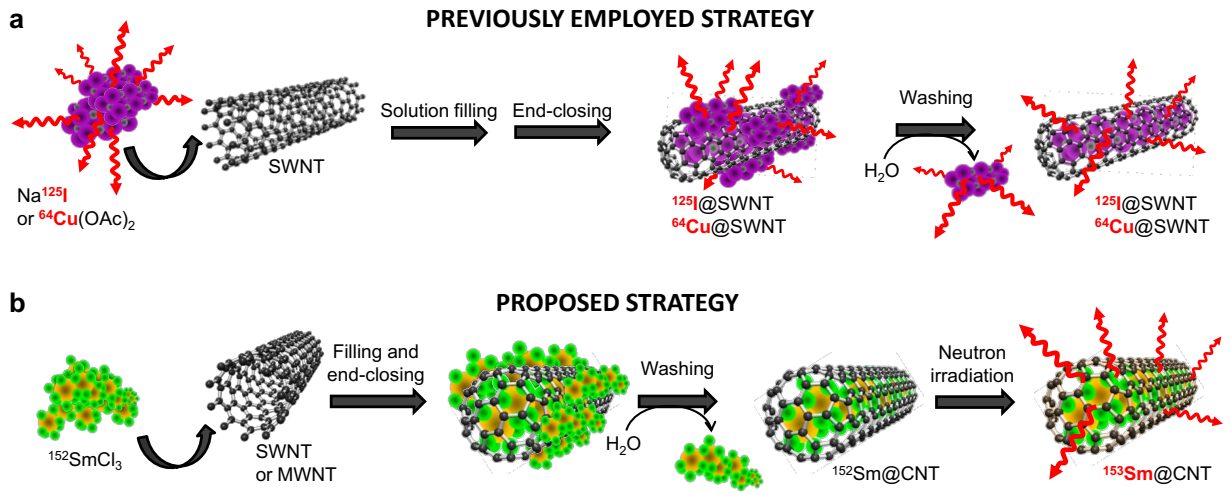

Figure S1. Schematic representation of the strategies employed for the hermetic sealing of radionuclides into the cavities of carbon nanotubes (hot nanocapsules). a) Previously employed strategies where radionuclides (^{125}I and ^{64}Cu) are directly filled into carbon nanotubes[1, 2]. b) Present strategy, also depicted in Fig. 1a (main text), where a non-radioactive enriched precursor is initially encapsulated (^{152}Sm) and it is activated into its radioactive form by neutron irradiation (^{153}Sm) in the last step. In both schematic representations, the wavy lines indicate radioactivity emerging from radionuclides (highlighted in the text in red).

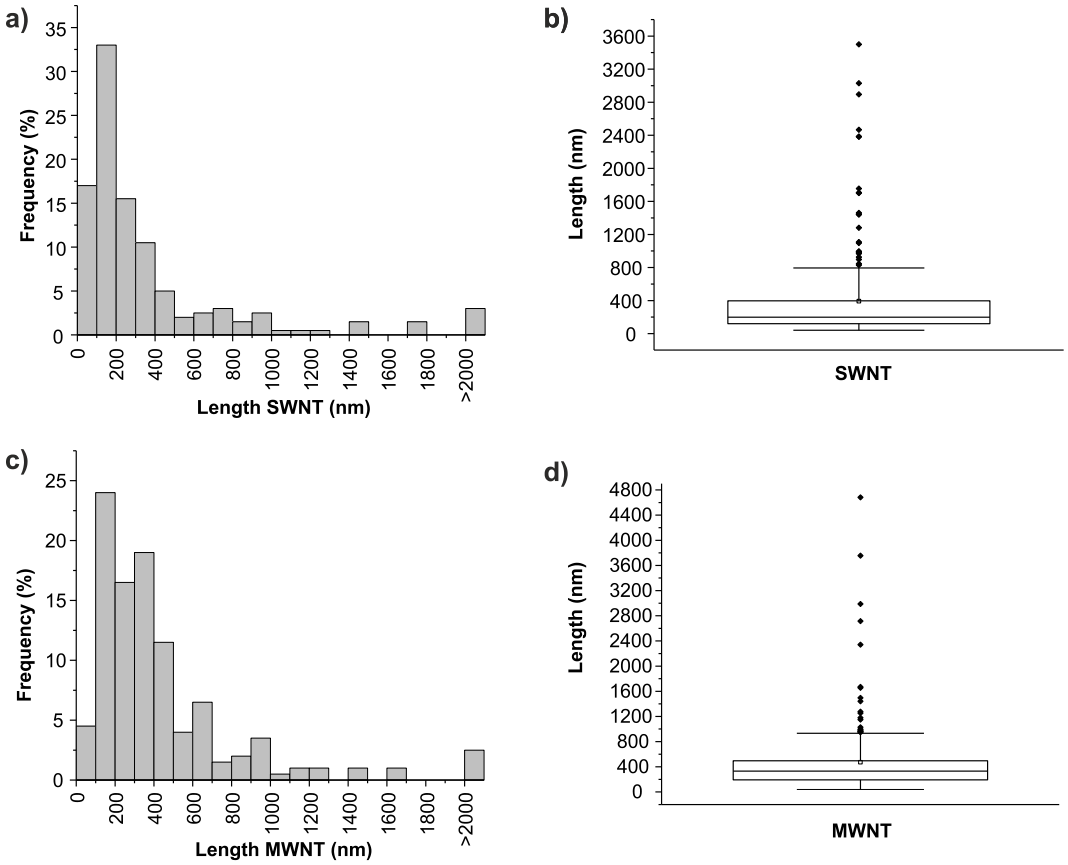

Figure S2. Length distribution of ^{152}Sm@CNT samples. a) Length distribution histogram and b) box plot analysis of SWNT; c) Length distribution histogram and d) box plot analysis of MWNT.

Table S1. Descriptive analysis of the length distribution of ^{152}Sm@CNT samples.

	N Number of measured CNT	Median (nm)	Lower observation (nm)	Lower adjacent observation (nm)	Q1 25th percentile (nm)	Q3 75th percentile (nm)	Maximum adjacent observation (nm)	Maximum observation (nm)
SWNT	200	199	41	41	120	397	794	3500
MWNT	200	331	40	40	192	495	932	4682

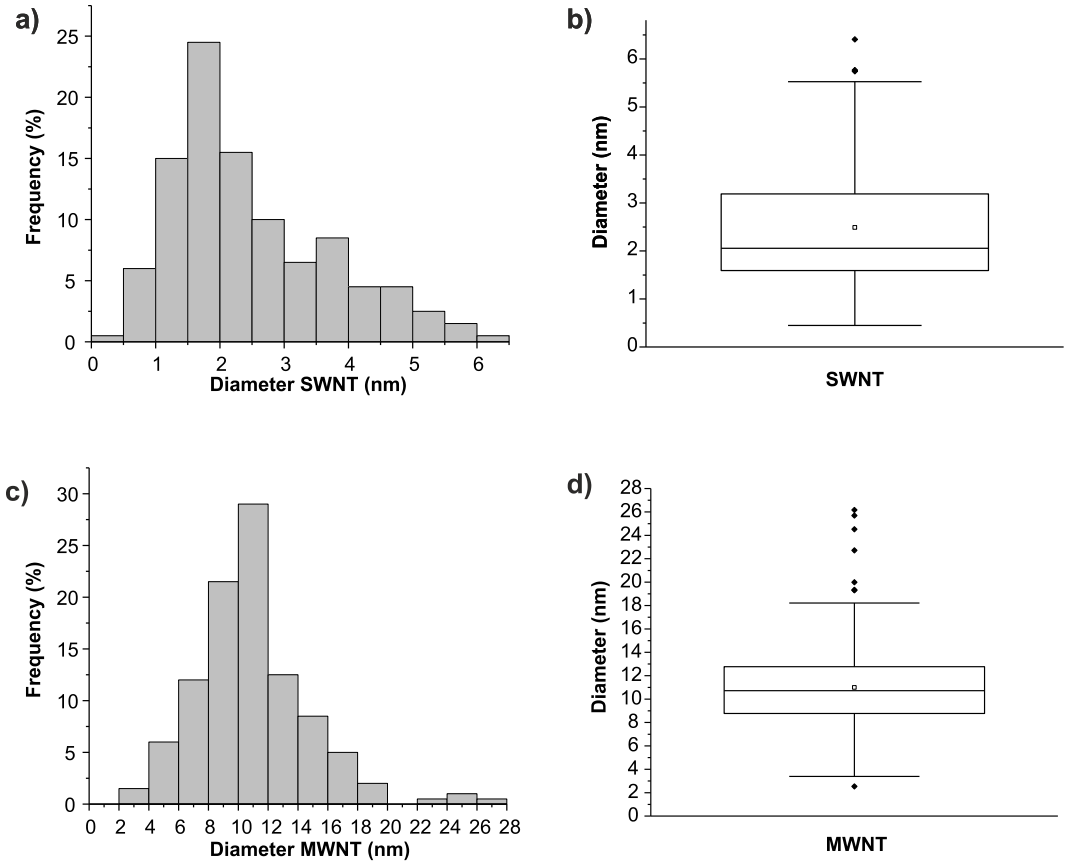

Figure S3. External diameter distribution of ^{152}Sm@CNT samples. a) Diameter distribution histogram and b) box plot analysis of SWNT; c) Diameter distribution histogram and d) box plot analysis of MWNT.

Table S2. Descriptive analysis of the external diameter distribution of ^{152}Sm@CNT samples.

	N Number of measured CNT	Median (nm)	Lower observation (nm)	Lower adjacent observation (nm)	Q1 25^{th} percentile (nm)	Q3 75^{th} percentile (nm)	Maximum adjacent observation (nm)	Maximum observation (nm)
SWNT	200	2.1	0.5	0.5	1.6	3.2	5.5	6.4
MWNT	200	10.7	2.5	3.4	8.8	12.8	18.2	26.2

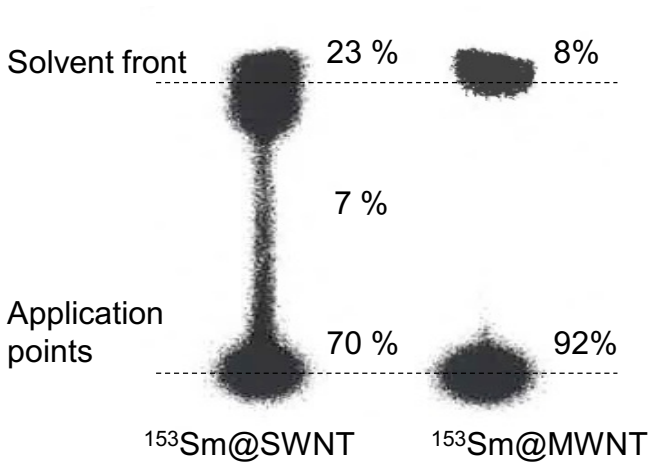

Figure S4. ITLC analysis of ^{153}Sm@SWNT and ^{153}Sm@MWNT following neutron irradiation of ^{152}Sm@SWNT and ^{152}Sm@MWNT respectively. Signals at the application point represent the stably encapsulated radionuclides.

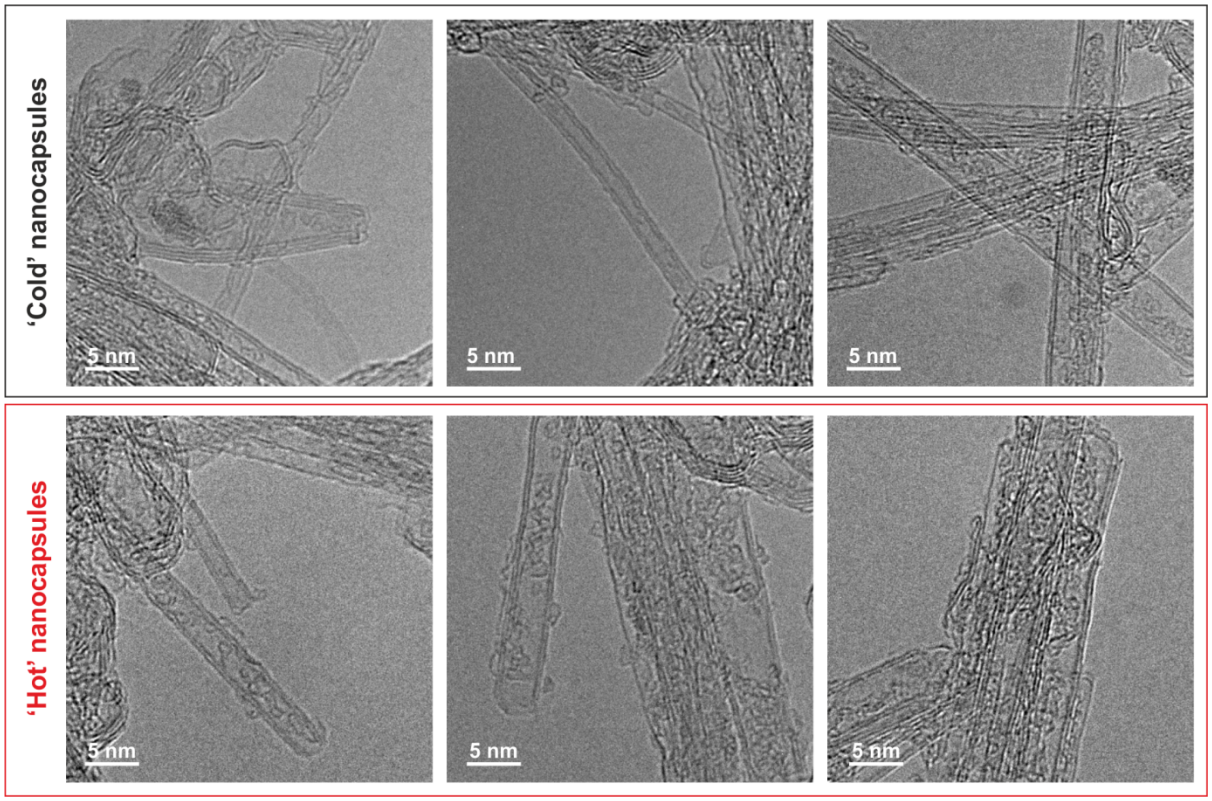

Figure S5. HRTEM images of Sm-filled SWNTs before ('Cold' nanocapsules) and after ('Hot' nanocapsules) irradiation.

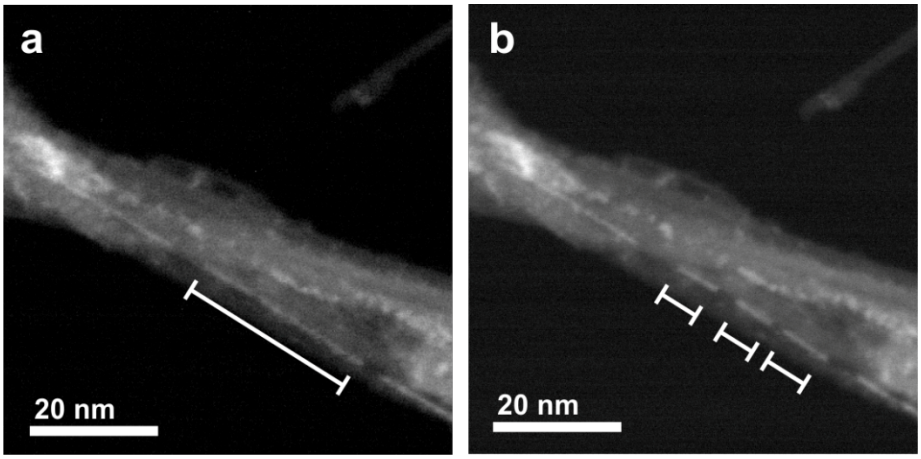

Figure S6. HAADF STEM images of a $^{152}SmCl_3$@SWNT showing that during electron microscopy observation the filling material displaces inside the SWNT. a) Initially acquired image and b) an image of the same area acquired after ca. 30 seconds. Displacement of the filling material is indicated with white bars.

Table S3. Neutron activated isotopes (of clinical interest) loaded onto nanocarriers.

Nanocarrier	Stable isotope	Neutron irradiation time	Neutron flux ($n \cdot cm^{-2} \cdot s^{-1}$)	Reported radioactivity[a]	Specific radioactivity[b] (MBq/mg)	Ref.
MWNT	^{152}Sm	96 h	$1.6x10^{14}$	11.37 GBq/mg	11370.0	This work
SWNT	^{152}Sm	96 h	$1.6x10^{14}$	6.33 GBq/mg	6330.0	This work
C_{82}	^{165}Ho	1 min	$4.3x10^{14}$	16.13 μCi/mg	0.6	3
MCN	^{165}Ho	10 h	$5.5x10^{12}$	208 μCi/100 μg	77.0	4
HoIG	^{165}Ho	0.45 h	$7.0x10^{12}$	250 μCi/mg	9.3	5
Silica NPs	^{165}Ho	1 h	$3.5x10^{12}$	213.6 μCi/mg	7.9	6
Silica NPs	^{165}Ho	2.2 h[c]	$5.5x10^{12}$	129 MBq/10.7 mg	12.1	7
Silica NPs	^{165}Ho	2 h	$5.5x10^{12}$	150 μCi/mg	5.6	8
Silica NPs	^{165}Ho	3 h	$7.7x10^{12}$	300 μCi/mg	11.1	8
AcAc	^{165}Ho	13 min	$5.5x10^{12}$	0.25 mCi/10 mg	0.9	9
AcAc	^{165}Ho	1 h	5.0×10^{12}	600 MBq/50 mg	12.0	10
PLLA	^{165}Ho	1 h	1.1×10^{13}	27.4 GBq/g	27.4	11

MWNT: Multi-walled carbon nanotubes; SWNT: Single-walled carbon nanotubes; C_{82}: Endohedral Metallofulerenes; HoIG: Holmium iron garnet; NPs: Nanoparticles; MCN: Mesoporous carbon nanoparticles; AcAc: NPs from acetylacetonate; PLLA: Poly-L-lactide

NOTES: [a]Values as reported in the reference provided

[b]Specific radioactivities calculated from "Reported activity"

[c]Irradiation up to 18h was performed but the resulting activity is not reported

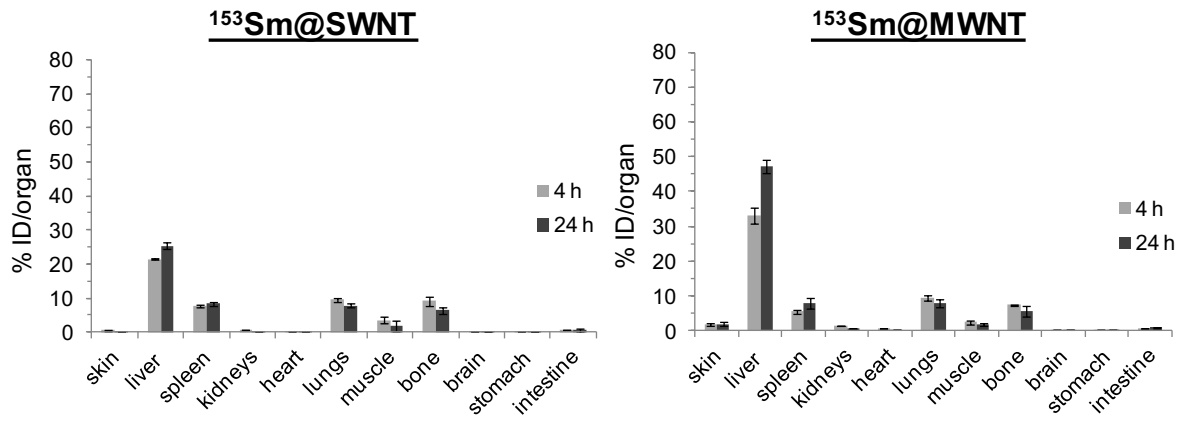

Figure S7. Tissue biodistribution of ^{153}Sm@SWNT and ^{153}Sm@MWNT (presented as %ID per organ). C57/Bl6 mice were i.v. injected with 200 μg of ^{153}Sm@SWNT or ^{153}Sm@MWNT (~1 MBq). The radioactivity of major organs sampled at specified time points were measured by γ-scintigraphy. The results are expressed as % ID/organ and presented as mean ± S.D. (n=3-4).

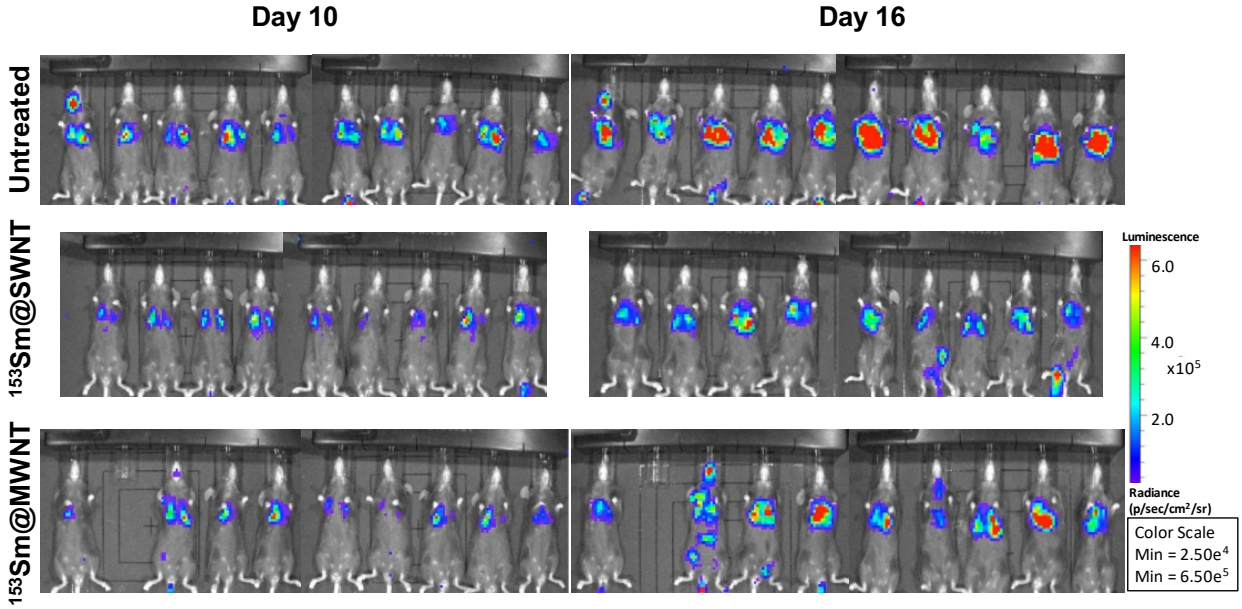

Figure S8. Live bioluminescence images of untreated mice or mice treated with ^{153}Sm@SWNT or ^{153}Sm@MWNT. B16F10-Luc tumor-bearing mice were i.v. injected with 20 MBq in 200 μg of ^{153}Sm@SWNT or ^{153}Sm@MWNT on day 8 post-tumor inoculation. Bioluminescence signals correspond to metabolic activity of luciferase-expressing B16F10 cells in the lung.

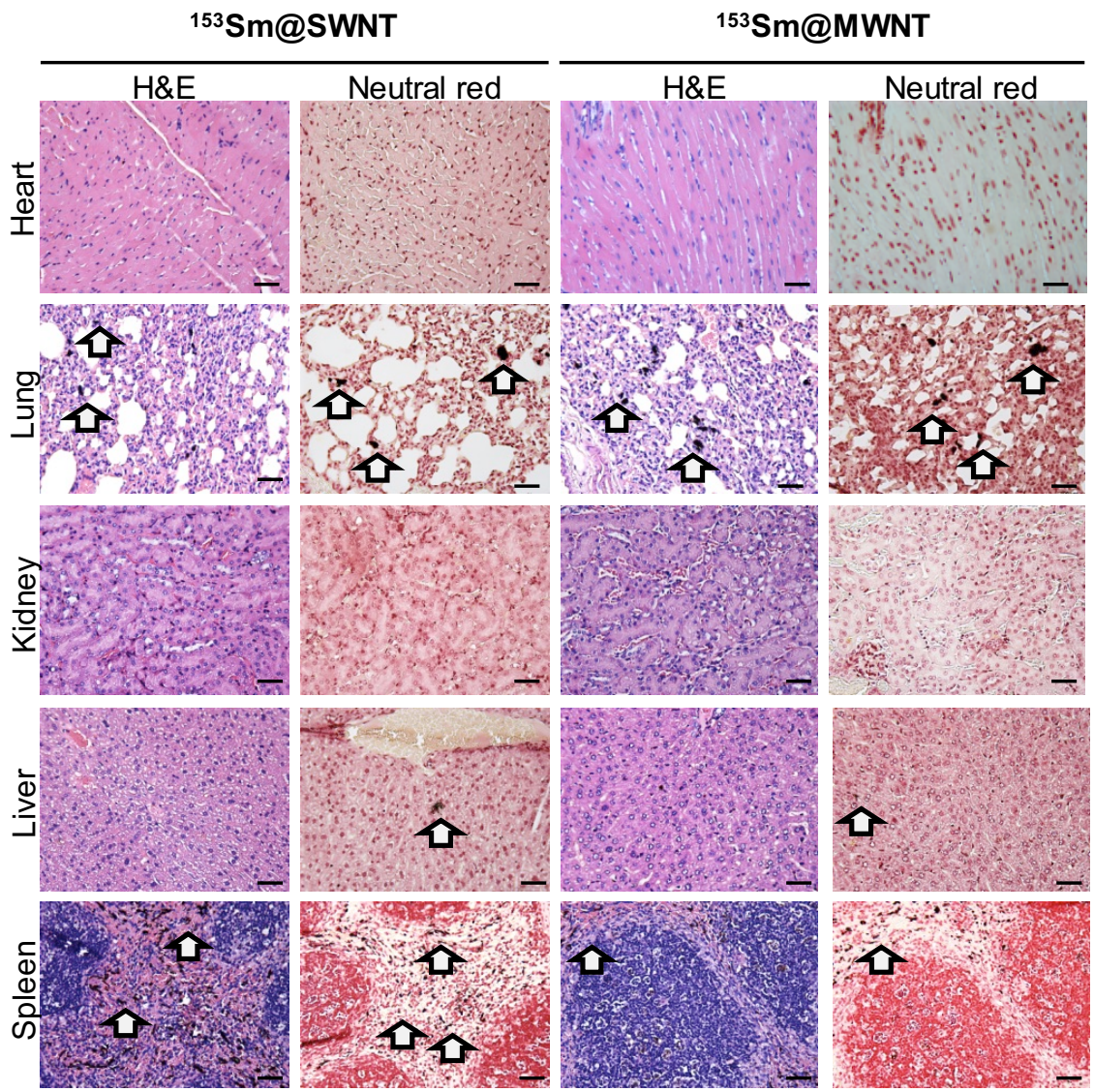

Figure S9. Histological examination of major organs from C57BL/6 mice at 24 h post injection of ^{153}Sm@SWNT and ^{153}Sm@MWNT. C57BL/6 mice were i.v. injected with 200 μg of ^{153}Sm@SWNT or ^{153}Sm@MWNT (~1 MBq). At 24 h post injection, heart, lung, kidney, liver, and spleen were excised and formalin-fixed, stained with H&E (for tissue necrosis) or Neutral Red (for CNT visualization). As a guide to the eye arrows point to some CNT aggregates. Scale bars: 50 μm.

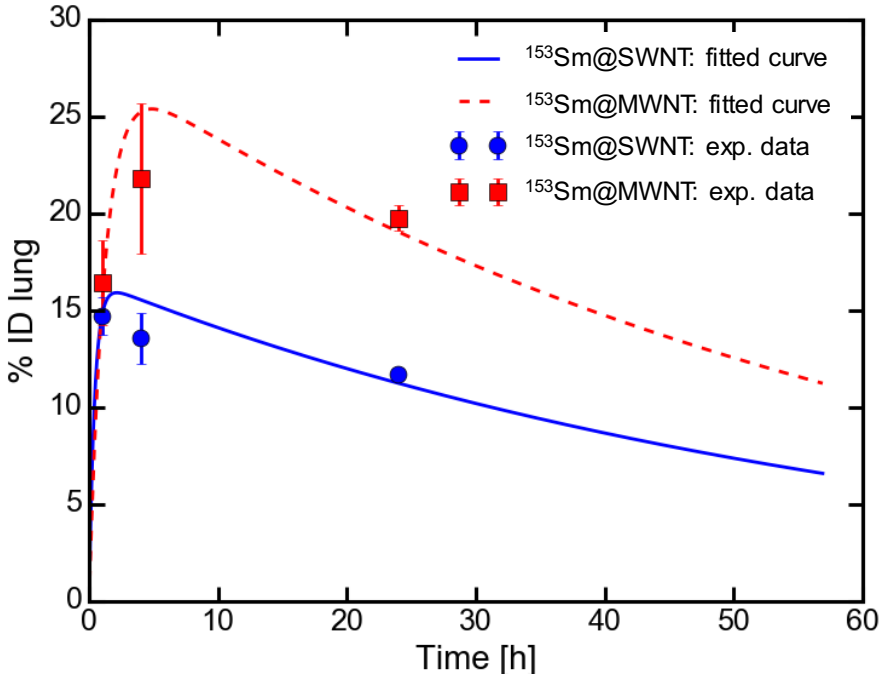

Figure S10. Fit of the experimental biodistribution data (% ID) in the lung using equation 3 described in the manuscript. Fitted parameters are $\mathrm{ID}_0 = 16.6\,\%$, $k = 0.0162\,\mathrm{h}^{-1}$ $m = 2.32\,\mathrm{h}^{-1}$ for SWNT, and $\mathrm{ID}_0 = 28.0\,\%$, $k = 0.0160\,\mathrm{h}^{-1}$ $m = 0.826\,\mathrm{h}^{-1}$ for MWNT. Experimental data are presented by circle or square dots. Lines (solid or dotted) are the fitted curve calculated using equation 3.

Experimental Details

Materials and Reagents: Chemical vapor deposition (CVD) Elicarb® SWNTs and MWNTs were supplied by Thomas Swan & Co. Ltd (UK) as a solid powder. The SWNT material also contains a fraction of few-walled carbon nanotubes, mainly double-walled. Enriched $^{152}Sm_2O_3$ were provided by CIS-Bio International-Ion Beam Applications (France). Hydrogen peroxide, sulphuric acid and nitric acids were purchased from Panreac AppliChem (Spain) for CNT pre-treatment. Instant thin layer chromatography paper impregnated with silica gel (ITLC-SG) was obtained from Agilent Technologies (UK). Isoflurane for anesthesia was purchased from Abbott (IsoFlo®, Abbott Laboratorie Ltd, UK).

Purification and Shortening of CNTs: Both SWNTs and MWNTs were initially treated to shorten the tubes, open their ends and remove carbonaceous and metallic (catalyst) impurities. SWNTs were exposed to a combined piranha-steam treatment, whereas MWNTs underwent a combined H_2SO_4:HNO_3-steam treatment following previously reported protocols.[12]

Synthesis of $^{152}SmCl_3$ from $^{152}Sm_2O_3$: Enriched $^{152}Sm_2O_3$ was transformed to anhydrous $^{152}SmCl_3$ following the protocol reported for the synthesis of anhydrous $SmCl_3$ with natural isotopic distribution (non-enriched).[13] The synthesis of the anhydrous metal halide was performed by dissolution of the enriched metal oxide in HCl, followed by dehydration of the collected solid at 240 °C under dynamic vacuum. The synthesized anhydrous $^{152}SmCl_3$ is highly hygroscopic and was handled under an inert atmosphere.

Filling of CNTs with $^{152}SmCl_3$: Cut and purified SWNT (100 mg) or MWNT (200 mg) and $^{152}SmCl_3$ were ground together in a weight ratio 1:10 (CNTs:$^{152}SmCl_3$). The materials were ground using an agate mortar and pestle inside an argon filled glove box until the mixture presented a uniform color. The samples were split in smaller fractions, placed inside silica tubes and sealed under vacuum. The resulting silica ampoules were placed inside a horizontal tubular furnace and annealed for 12 h at 900 °C (SWNT) or 1200 °C (MWNT) thus leading to the formation of carbon nanocapsules (closed-ended filled CNTs). The samples were recovered from the ampoules and the non-encapsulated material, external to the CNTs was dissolved and washed away. The removal of the external material was followed by UV-Vis spectroscopy of the

collected filtrates, until no more $^{152}SmCl_3$ was detected in the washings.[14] Initially the filled nanotubes were soaked in 200 mL of water containing 0.6 M HCl. The sample was then collected by filtration over a 0.2 μm polycarbonate membrane. This "pre-washing" step was followed by washing the sample three times in 200 mL acidic water at 80 °C for 24 h under constant stirring each time. The sample was collected by filtration between washings. A final washing step was performed using 200 mL of pure water, without the addition of HCl, whilst keeping the rest parameters constant. The collected solid powder was dried at 80 °C overnight.

Neutron activation of ^{152}Sm-filled CNTs: Vacuum sealed silica ampoules containing 30 mg of either ^{152}Sm@SWNT or ^{152}Sm@MWNT were placed in an aluminum capsule, weighed down with a lead-weight in a pool-type reactor (OSIRIS, CEA Saclay, France) and irradiated at a neutron flux of $1.6x10^{14}$ n·cm^{-2}·s^{-1} for 96 h. The irradiation protocol was established according to equation (1):[15]

$$A = \frac{0.6\sigma\Phi}{M}\left(1 - e^{-\lambda t}\right) \qquad (1)$$

where A is the predicted activity of the radioisotope produced (Bq g^{-1}), M is the atomic mass of the target element (152 g mol^{-1} for ^{152}Sm), Φ is the neutron flux of the reactor ($1.6x10^{14}$ n cm^{-2}s^{-1}), σ is the thermal neutron activation cross-section of the target isotope (206 barns for ^{153}Sm), λ is the decay constant ($0.693/T_{1/2}$), ($T_{1/2}$ is the half life of the target isotope, which is 46.27 h for ^{153}Sm) and *t* is the irradiation time (96 h). The value of A for the given conditions can then be used to make a prediction of the nanotubes, by factoring in the mass of nanotubes and the corresponding percentage content of ^{152}Sm that was measured before the irradiation.

After removing the ampoules from the pool, they were allowed to cool down, removed from the aluminum casing, and then transferred to CIS bio International, Saclay (France) where they were processed in a fully sealed radioprotection hot cell. Radioactivity was measured using a dose calibrator (VDC 404, Veenstra Instruments, The Netherlands). The ampoules were then shattered and the contents (^{153}Sm@SWNT and ^{153}Sm@MWNT powders) were separately suspended in a volume of 1% Pluronic® F-127 saline (0.9 % NaCl) solution, using sonication such to produce a suspension with a loading of 0.5 mg/mL. The glass fragments from the broken silica ampoule were separated from the bulk of the suspension by sedimentation. Large aggregates of ^{153}Sm@CNTs were also precluded in this way. In order to transfer this product to the *in vivo*

facilities in vials, keeping within their local limits of activity handling, only a fraction of this suspension was then separated into a final vial, which was then shipped and arrived in a few days. On arrival, a sonication and a series of dilution steps were performed to ensure that the final dispersion injected in mice was physically stable and free of aggregates, as detailed in the *in vivo* section.

Quantification of $^{152}SmCl_3$ filling yields by ICP-MS: As a analytical validation measure, each carbon nanotube sample was subdivided into fractions of different sizes in the range of 1-15 mg, and was weighed three times on a pre-calibrated analytical balance. The samples were then added to a PTFE-TFM reactor in an Anton Paar Multiwave 3000, fitted with an 8SXF100 rotor. 6 mL 65% Suprapur® nitric acid (Merck KGaA, Germany), and then 2 mL of 30% Suprapur® hydrogen peroxide (Merck KGaA, Germany) were dispensed from calibrated micropipettes and the microwave digestion was completed by applying 800 W for 40 minutes, with an initial ramp of 5 min. The contents of each reactor were then transferred to a polyproylene flask, followed by a series of washings with de-ionised water (ELGA Labwater PURELAB® Classic water purifying system; resistivity 18.2 MΩ/cm), and the volume was then made up to 25 mL. Two additional control solutions were prepared and analyzed. It was demonstrated that no impurities were introduced during this process using a "preparation blank," consisting of all of the reagents except the nanotubes, that was passed through the microwave at the same time as the actual samples. It was also confirmed that all of the material that was added to the reactors was recovered by preparing a solution from the final washing. Prior to analysis by ICP-MS, all of the samples were filtered with a 33 mm 0.22 μm MILLEX ® GV PVDT filter.

ICP-MS analysis was carried out at Cis Bio International using an ICP-MS with a quadrupole collision cell (PerkinElmer Sci EX ELAN® DRC II). The system check consisted of: a daily performance report using a standard reference solution of magnesium, indium, uranium, cerium and barium, with relative standard deviations (RSD) within 0.4 to 1.1% of the anticipated value. The sample sequence then consisted of triplicate injections of: a blank containing de-ionized water, the "preparation blank" and then the actual samples, separated by injections of de-ionized water. The quantification was performed using an external ^{152}Sm calibration standard. The stability of the measurements was monitored by spiking each sample with an identical level of a rhodium standard of 5 ppb and this gave RSDs of less than 1%. The range of concentrations

chosen for the ^{152}Sm calibration depended on the particular sample and covered the ranges of either 1 to 5 ppb or 1 to 30 ppb, and all of Pearson correlation coefficients R^2 coefficients were greater than 0.9999. The results corresponding to the overall % ^{152}Sm were then reported to one decimal place.

Electron microscopy: HAADF-STEM images were acquired at 20 kV on an FEI Magellan XHR Scanning Electron Microscope (SEM) with the use of a specially adapted detector. HRTEM images were acquired on a FEI Tecnai G2 F20 microscope at 200 kV. Samples were dispersed in ethanol and deposited onto lacey carbon Cu grids. ^{153}Sm@CNT were imaged after the complete decay of radioactivity. EDX was carried out on a FEI Quanta SEM microscope equipped with an EDAX detector at 20 kV.

Animals: All *in vivo* experiments were conducted under the authority of project and personal licenses granted by the UK Home Office and the UKCCCR Guidelines (1998). Female C57BL/6 mice aged 6-8 weeks were purchased from Harlan (UK) and used for all *in vivo* studies.

ITLC examination of ^{153}Sm@CNTs: ITLC was performed to examine whether there was free ^{153}Sm present in the ^{153}Sm@CNT suspensions (neutron irradiated ^{152}Sm@CNT) prior to injection. Aliquots of ^{153}Sm@SWNT and ^{153}Sm@MWNT were spotted on TLC strips and then developed in 0.1 M ammonium acetate containing 50 mM EDTA as a mobile phase. Strips were allowed to dry and counted quantitatively using a cyclone phosphor detector (Packard Biosciences, UK).

Preparation of ^{153}Sm-CNTs for in vivo studies: The ^{153}Sm@CNT suspensions underwent different dilutions to contain the appropriate radioactivity for different *in vivo* studies. The dilution was carried out by mixing the ^{153}Sm@CNT dispersions with different amounts of non-irradiated ^{152}Sm@CNT suspensions (2 mg/mL in 1% Pluronic® F-127 saline). The resulting mixture was then sonicated for 10-15 min. Each injection dose, either for imaging, biodistribution or therapy studies, contained the same amount of CNT (200 μg), but possessed different radioactivity which are specified in their experimental sections accordingly. Injection suspensions were added with 0.1 M EDTA (one twentieth of the injection volume) to chelate any free ^{153}Sm.

In vivo SPECT/CT imaging of ^{153}Sm@CNT following i.v. injection: The biodistribution of ^{153}Sm@CNTs was firstly assessed by 3D whole body SPECT/CT imaging. Mice were anaesthetized by isoflurane inhalation during imaging. Each injection dose for ^{153}Sm@SWNT or

^{153}Sm@MWNT suspensions contained approximately 10 MBq. Injection suspensions were added with 0.1 M EDTA (one twentieth of the injection volume) to chelate free ^{153}Sm. Immediately after injection, and at 4 h and 24 h, mice were imaged using the Nano-SPECT/CT scanner (Bioscan, USA). SPECT images of each mouse were taken in 24 projections over 30-40 min using a four-head scanner with 1.4 mm pinhole collimators. CT scans were performed at the end of each SPECT acquisition. All images were reconstructed by MEDISO software (Medical Imaging Systems), and SPECT and CT images were merged using the InVivoScope™ software (Bioscan, USA).

Pharmacokinetics and organ biodistribution of ^{153}Sm@CNTs by γ-scintigraphy: Mice anaesthetized by isoflurane inhalation were injected with ^{153}Sm@SWNT or ^{153}Sm@MWNT suspensions *via* a tail vein. Each injection dose of ^{153}Sm@SWNT or ^{153}Sm@MWNT suspensions contained approximately 0.8 MBq. Blood was sampled from a tail vein at 5 min, 30 min, 4 h or 24 h after injection. At 4 h and 24 h, mice were sacrificed and major organs were excised and weighed. To assess the excretion profiles, animals were housed individually in metabolic cages where the mice have free access to water but not food. Urine and feces were collected over 24 h after injection. The radioactivity of each sample (*i.e.* tissues, blood, urine or feces) was measured by γ-scintigraphy (LKB Wallac 1282 Compugamma, PerkinElmer) and the results were expressed as percentage injection dose per sample (% ID) or per g of sample (% ID/g). Collected organs were fixed in 10% neutral buffered formalin for histological examination.

B16F10-Luc lung metastasis tumor model: Mice anaesthetized by isoflurane inhalation were injected with 5 x 10^5 B16F10-Luc cells in 0.2 mL of PBS *via* a tail vein to establish pulmonary melanoma metastases. Following tumor inoculation, *in vivo* quantitative bioluminescence imaging was performed on day 7, 10, 13 and 16 to monitor the tumor growth (IVIS Lumina III, Perkin-Elmer, UK). Mice under anesthesia were subcutaneously injected with luciferin (D-luciferin potassium salt, Perkin-Elmer, UK) at 150 mg/kg and imaged 10 min after injection. Bioluminescence signals from regions of interests were measured using Living Image software (Perkin-Elmer, UK) and recorded as total flux (photons/sec).

In vivo ^{153}Sm@CNT radiotherapy studies: To determine the radiotherapeutic action of ^{153}Sm@SWNT and ^{153}Sm@MWNT, B16F10-Luc tumor bearing C57BL/6 mice were randomly divided into three groups (n = 10): untreated, ^{153}Sm@SWNT and ^{153}Sm@MWNT. On day 8 post

tumor inoculation, mice were intravenously injected with 200 μg of ^{153}Sm@SWNT or ^{153}Sm@MWNT suspensions containing approximately 20 MBq. Mice were sacrificed on day 16 post tumor inoculation, and major organs including lung, liver, spleen, heart, and kidney were weighed and fixed in 10% neutral buffered formalin for histological examination. Tumor growth was monitored by bioluminescence imaging as described previously. The tumor growth data was expressed as mean ± SEM (standard error of the mean), with *n* denoting the number of animals. Significant differences were examined using one-way ANOVA followed by Tukey's multiple comparison test. *: $p < 0.05$; ***: $p < 0.001$

Histological examination: Major organs excised from the mice in the biodistribution study (*i.e.* 24 h post injection) and from the mice after ^{153}Sm@CNT radiotherapy were subjected to histological examination. Harvested fixed organs were paraffin-embedded and sectioned for haematoxylin and eosin (H&E) or Neutral Red staining according to standard histological protocols at the Royal Veterinary College (UK). All stained sections were analysed using a Leica DM 1000 LED Microscope (Leica Microsystems, UK) coupled with a CCD digital camera (Qimaging, UK).

References

1. Hong, S. Y.; Tobias, G.; Al-Jamal, K. T.; Ballesteros, B.; Ali-Boucetta, H.; Lozano-Perez, S.; Nellist, P. D.; Sim, R. B.; Finucane, C.; Mather, S. J.; Green, M. L. H.; Kostarelos, K.; Davis, B. G. Filled and Glycosylated Carbon Nanotubes for *In Vivo* Radioemitter Localization and Imaging. *Nat. Mater.* **2010**, *9*, 485-490.
2. Ge, H.; Riss, P. J.; Mirabello, V.; Calatayud, D. G.; Flower, S. E.; Arrowsmith, R. L.; Fryer, T. D.; Hong, Y.; Sawiak, S.; Jacobs, R. M. J.; Botchway, S. W.; Tyrrell, R. M.; James, T. D.; Fossey, J. S.; Dilworth, J. R.; Aigbirhio, F. I.; Pascu, S. I. Behavior of Supramolecular Assemblies of Radiometal-Filled and Fluorescent Carbon Nanocapsules *In Vitro* and *In Vivo*. *Chem* **2017**, *3*, 437-460.
3. Cagle, D. W.; Kennel, S. J.; Mirzadeh, S.; Alford, J. M.; Wilson, L. J. *In Vivo* Studies of Fullerene-Based Materials Using Endohedral Metallofullerene Radiotracers. *Proc. Natl. Acad. Sci. U. S. A.* **1999**, *96*, 5182-5187.
4. Kim, J.; Luo, Z.-X.; Wu, Y.; Lu, X.; Jay, M. *In-Situ* Formation of Holmium Oxide in Pores of Mesoporous Carbon Nanoparticles as Substrates for Neutron-Activatable Radiotherapeutics. *Carbon* **2017**, *117*, 92-99.
5. Munaweera, I.; Shi, Y.; Koneru, B.; Saez, R.; Aliev, A.; Di Pasqua, A. J.; Balkus, K. J. Chemoradiotherapeutic Magnetic Nanoparticles for Targeted Treatment of Nonsmall Cell Lung Cancer. *Mol. Pharm.* **2015**, *12*, 3588-3596.

6. Munaweera, I.; Koneru, B.; Shi, Y.; Pasqua, A. J. D.; Kenneth J. Balkus, J. Chemoradiotherapeutic Wrinkled Mesoporous Silica Nanoparticles for Use in Cancer Therapy. *APL Mater*. **2014**, *2*, 113315.
7. Di Pasqua, A. J.; Yuan, H.; Chung, Y.; Kim, J. K.; Huckle, J. E.; Li, C.; Sadgrove, M.; Tran, T. H.; Jay, M.; Lu, X. Neutron-Activatable Holmium-Containing Mesoporous Silica Nanoparticles as a Potential Radionuclide Therapeutic Agent for Ovarian Cancer. *J. Nucl. Med*. **2013**, *54*, 111-116.
8. Di Pasqua, A. J.; Miller, M. L.; Lu, X.; Peng, L.; Jay, M. Tumor Accumulation of Neutron-Activatable Holmium-Containing Mesoporous Silica Nanoparticles in an Orthotopic Non-Small Cell Lung Cancer Mouse Model. *Inorg. Chim. Acta* **2012**, *393*, 334-336.
9. Di Pasqua, A. J.; Huckle, J. E.; Kim, J.-K.; Chung, Y.; Wang, A. Z.; Jay, M.; Lu, X. Preparation of Neutron-Activatable Holmium Nanoparticles for the Treatment of Ovarian Cancer Metastases. *Small* **2012**, *8*, 997-1000.
10. Bult, W.; Varkevisser, R.; Soulimani, F.; Seevinck, P. R.; de Leeuw, H.; Bakker, C. J. G.; Luijten, P. R.; van het Schip, A. D.; Hennink, W. E.; Nijsen, J. F. W. Holmium Nanoparticles: Preparation and *In Vitro* Characterization of a New Device for Radioablation of Solid Malignancies. *Pharm. Res*. **2010**, *27*, 2205-2212.
11. Hamoudeh, M.; Fessi, H.; Salim, H.; Barbos, D. Holmium-Loaded PLLA Nanoparticles for Intratumoral Radiotherapy *via* the TMT Technique: Preparation, Characterization, and Stability Evaluation after Neutron Irradiation. *Drug Dev. Ind. Pharm*. **2008**, *34*, 796-806.
12. Kierkowicz, M.; Pach, E.; Santidrián, A.; Sandoval, S.; Gonçalves, G.; Tobías-Rossell, E.; Kalbáč, M.; Ballesteros, B.; Tobias, G. Comparative Study of Shortening and Cutting Strategies of Single-Walled and Multi-Walled Carbon Nanotubes Assessed by Scanning Electron Microscopy. *Carbon* **2018**, *139*, 922-932.
13. Martincic, M.; Frontera, C.; Pach, E.; Ballesteros, B.; Tobias, G. Synthesis of Dry $SmCl_3$ from Sm_2O_3 Revisited. Implications for the Encapsulation of Samarium Compounds into Carbon Nanotubes. *Polyhedron* **2016**, *116*, 116-121.
14. Martincic, M.; Pach, E.; Ballesteros, B.; Tobias, G. Quantitative Monitoring of the Removal of Non-Encapsulated Material External to Filled Carbon Nanotube Samples. *Phys. Chem. Chem. Phys*. **2015**, *17*, 31662-31669.
15. *Manual for Reactor Produced Radioisotopes, Iaea-Tecdoc-1340*. Vienna, Austria, **2003**, 189-192.